*Retraction*

# Retracted: Display and Analysis of Virtual 3D Technology in Interior Design

## Journal of Sensors

This article has been retracted by Hindawi following an investigation undertaken by the publisher [1]. This investigation has uncovered evidence of one or more of the following indicators of systematic manipulation of the publication process:

(1) Discrepancies in scope

(2) Discrepancies in the description of the research reported

(3) Discrepancies between the availability of data and the research described

(4) Inappropriate citations

(5) Incoherent, meaningless and/or irrelevant content included in the article

(6) Manipulated or compromised peer review

The presence of these indicators undermines our confidence in the integrity of the article's content and we cannot, therefore, vouch for its reliability. Please note that this notice is intended solely to alert readers that the content of this article is unreliable. We have not investigated whether authors were aware of or involved in the systematic manipulation of the publication process.

Wiley and Hindawi regrets that the usual quality checks did not identify these issues before publication and have since put additional measures in place to safeguard research integrity.

We wish to credit our own Research Integrity and Research Publishing teams and anonymous and named external researchers and research integrity experts for contributing to this investigation.

The corresponding author, as the representative of all authors, has been given the opportunity to register their agreement or disagreement to this retraction. We have kept a record of any response received.

## References

[1] L. Sen and L. Yang, "Display and Analysis of Virtual 3D Technology in Interior Design," *Journal of Sensors*, vol. 2023, Article ID 2231483, 10 pages, 2023.

Hindawi

*Research Article*

# Display and Analysis of Virtual 3D Technology in Interior Design

**Liu Sen** [1] **and Liu Yang** [2]

$^{1}$*BaoDing University, HeBei, Baoding 071000, China*
$^{2}$*Hebei College of Science and Technology, Baoding 071000, China*

Correspondence should be addressed to Liu Sen; liusen@bdu.edu.cn and Liu Yang; 524809747@qq.com

People are not satisfied with the two-dimensional technology, and three-dimensional virtual technology gradually enters every aspect of people's daily life: medical treatment, education, social interaction, vision, and so on. Virtual 3D technology brings a lot of convenience to people's lives and plays a core role in indoor scene design and layout. It enables users to see their own virtual indoor furniture and vegetation layout in advance and select and modify their own needs. We put forward several characteristics of indoor furniture selection and placement, such as no space restriction, interactivity and fault tolerance, and advanced display. We construct the basic algorithm of image transformation registration detection and finally optimize the basic algorithm with three different deep learning algorithm models, and get that the convolution layer neural network algorithm is superior to the other two models not only in the selection and placement of virtual furniture but also in the layout design of virtual vegetation landscape. Finally, for image defect detection, we compare the time cost of three models, which further shows that the convolution layer combined with image transformation technology model is fast and efficient.

## 1. Introduction

Virtual 3D technology is more and more widely used in our daily life, especially in architecture design, VR games, and humanities education. In different academic research, digital 3D technology in humanities education scene, community, and cognitive differences in several aspects carried out a good application value [1]. In addition to several 3D technology applications introduced above, virtual technology also plays a core value application in the development of games, combining campus real scene with virtual technology, so that students can feel the campus environment on the Internet [2]. In orthodontic treatment, facing the patient's ideal face, doctors should carry out 3D face detection on the patient and combine 3D imaging with modeling technology to give the patient an ideal treatment plan [3]. Many cultural relics in history have been damaged to varying degrees. Using 3D technology to restore cultural relics enables our future generations to reunderstand the exquisite technology and wisdom of ancestors at that time [4]. The Black Ding Bowl in Inner Mongolia was restored, and the restored appearance was obtained by virtual reconstruction

through 3D technology, and prosthetic materials were used for long-term preservation of cultural relics [5]. For animation design of ancient buildings in film and television works, it is necessary to set up the mutual unity of ancient buildings and characters according to the specific characters and environment at that time [6]. A series of operations for detection and resection of intracranial tumors need the support of three-dimensional technology, which can have a clear understanding of the size and location of tumors and improve the success rate of surgery [7]. In archaeological research, integrating 3D technology into archaeology can promote students' deep understanding of archaeology and full 3D reasoning, which runs through the whole archaeological process [8]. In the marine ecosystem, coral reef is an important part of maintaining the ecosystem. The structural restoration of damaged coral reef by 3D technology shows the expansibility of 3D model [9]. For the complex causes of dentists, such as adjacent supernumerary teeth, pulp tumor, and trauma, 3D virtual images are obtained by computed tomography (CT) technology, and replicas are generated by LCD-based mask stereolithography 3D printing technology [10]. For the practice teaching of congenital

heart disease, 3D printing and heart model combined with PBL technology are selected for teaching [11]. In the humanitarian social environment, for Africa and other countries with poor medical environment, 3D technology and telemedicine are used to provide medical assistance to patients under virtual technology. Our common 3D imaging is different from looking directly at images and videos with our ordinary eyes. For 2D imaging, the influence of 3D on human vision is convex instead of planar imaging [12, 13]. In the course of fashion design, students are taught to print 3D fashion products, make a prototype of 3D accessories, use computer-aided design to increase students' understanding of computer-aided design methods [14], use CAD and 3D technology to manufacture high-precision mechanical devices, build a low-temperature goniometer, and measure samples from different angles [15]. However, 3D printing technology also has an unbreakable difficulty, although it already has the advantages of high-precision printing to show smooth objects and fast printing speed [16]. The drug was prepared by 3D printing technology, and the coaxial scaffold with controllable tissue was used for long-term stable drug release [17]. In cosmetic surgery, 3D design is also applied to maxillofacial bone reconstruction surgery, which can be combined with anatomy, and 3D implantation increases the perfection of this kind of surgery [18]. In rhinoplasty, the simulated 3D image is converted into the operation plan of the operating room in a quantitative way, which is helpful to quantitatively translate the patient target in dorsal reduction rhinoplasty to the operating room and patients in the form of preoperative markers [19]. In the digital education space, the engineering thinking mode is used to formulate the principles and support directions of student research activity tutors in three-dimensional modeling [20]. The use of 3D printing technology in medicine is aimed at determining whether medical students are willing to use this technology to obtain accurate anatomical models to help them learn [21]. 3D printing is an increasingly feasible method, which can be used to customize the design and manufacture of assistive technologies. The evaluation of assistive technologies to be 3D printed should include information about individual activities, routines, skills, abilities, and preferences [22]. Ceramics can be replicated and mapped by 3D printing technology [23]. Children's dentition, jaw and facial growth, and development are disordered. The nasolabial angle and facial convex angle in the study group are significantly larger than those in the control group, and the difference is statistically significant [24]. Papers on multimodal data using spectral imaging and 3D technology in remote sensing, including new sensors, developing machine learning technology for data analysis, and the application of these technologies in various geospatial applications [25].

## 2. Virtual Scene Design

### 2.1. Basic Framework.
Virtual design of indoor scenes is a three-tier network architecture with server as the core, the expression layer is the user of virtual design scheme, and the architecture logic layer includes indoor virtual layout design, indoor virtual furniture design, and indoor virtual vegetation landscape layout. The data access layer is MySQL technology. The basic architecture of indoor virtual scene design and layout using VRML/X3D technology is shown in Figure 1.

### 2.2. Design and Layout Process of Indoor Scenes.
The virtual design of indoor scene needs to collect the customer's demand information firstly and draw up the general layout and modeling design of the scene according to the customer's demand. First, the basic configuration of each indoor scene is carried out, and then the specific integrated design of each area is carried out. The complete virtual design steps of indoor scene are as follows:

(1) Collect and sort out the customer's demand and feasibility analysis data, as well as the data needed to build indoor scenes

(2) Establish the basic layout model of indoor apartment, which includes ground model, wall model, door and window model, and furniture and vegetation landscape layout design for indoor scenes in each area

(3) Display the data of each basic model with three-dimensional graphics and see the preliminary building model

(4) The main network and network homepage will be constructed and connected with virtual files

(5) Finally, the complete virtual design result of indoor landscape is obtained

### 2.3. Features of Virtual Furniture.
Furniture is a necessary entity in a building house, and it takes time and effort for entities to enter the interior for on-site design. Therefore, the existence of the Internet has led to virtual furniture display, so that consumers can choose their favorite furniture without leaving home. The characteristics of virtual furniture display are as follows:

*(1) Not Limited by Space.* Virtual furniture in the indoor display can let consumers no matter where at what time can see the furniture entity in the indoor virtual display, which breaks the actual distance. The display of virtual furniture on the network can also show the scene to multiple customers at the same time, which can also improve the efficiency of customers' furniture selection, and the merchants can also obtain higher profits and achieve a win-win situation for both parties.

*(2) Interactivity and Fault Tolerance.* Virtual furniture can be selected according to their own preferences and placed indoors, and they will not interfere with other users' personalized design while choosing on the network. Users can also modify and adjust in real time in the virtual scene, which has great fault tolerance in furniture design. This makes furniture display more innovative and dynamic.

*(3) The Characteristics of Advanced Display.* The display of virtual furniture in indoor scenes can appear in the customer's field of vision in advance, and even if the furniture has not been produced, it can be purchased by customers
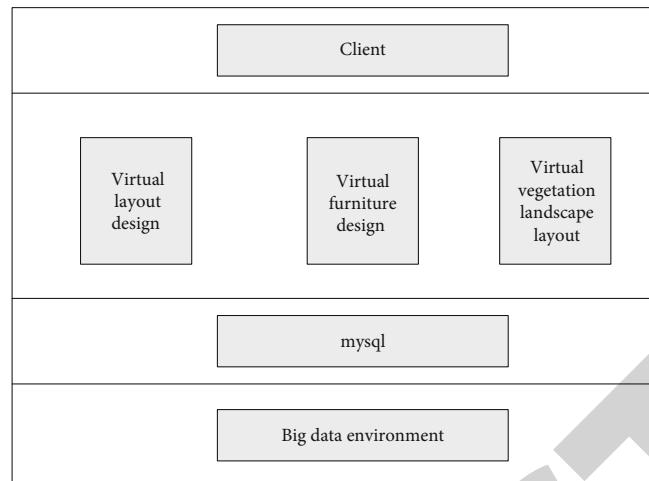
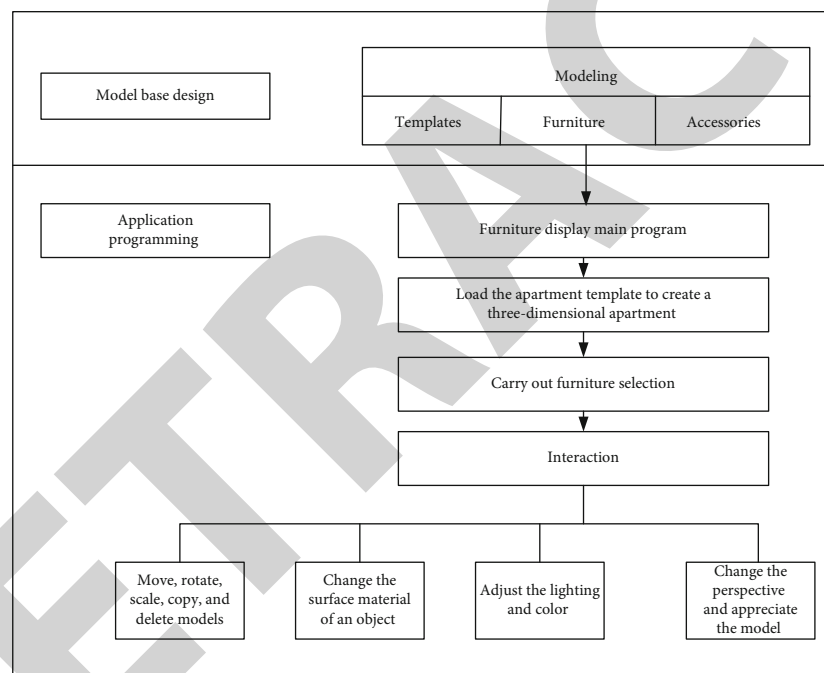FIGURE 1: Basic architecture of virtual scene design.



FIGURE 2: Framework of virtual furniture display system based on 3D modeling.

in advance. In this way, producers can quickly know which furniture customers like, and then mass-produce, so that they can clearly know the needs of customers.

The system framework of software model base design and program design for virtual furniture display is shown in Figure 2.

*(4) Energy Conservation and Environmental Protection.* Furniture for physical display will use materials that are not environmentally friendly, such as large spray-painted portraits and foam boards. Virtual furniture can reduce cost and environmental pollution and use virtual technology to help customers choose furniture, save energy, and achieve green environmental protection. VMware virtualization

solutions can reduce millions of tons of carbon dioxide emissions in the air, not only directly swing furniture for customers to choose but also greatly reduce labor costs.

The indoor display renderings of three different apartment types after being designed by virtual technology are shown in Figures 3–5:

## 3. Image Processing Algorithms

*3.1. Image Transformation.* The indoor spatial position is expressed by coordinate transformation.

$$\left(x', y'\right) = g(x, y). \tag{1}$$

FIGURE 3: Virtual design unit 1.



FIGURE 4: Virtual designer 2.

The expression that transforms the two-dimensional coordinates of the drawing of an indoor scene to $(x', y')$ through a rigid body at a certain point.

$$\begin{bmatrix} x' \\ y' \end{bmatrix} = \begin{bmatrix} \cos \varphi \pm \sin \varphi \\ \sin \varphi \mp \cos \varphi \end{bmatrix} \begin{bmatrix} x \\ y \end{bmatrix} + \begin{bmatrix} t_x \\ t_y \end{bmatrix}. \qquad (2)$$

An expression that affines the two-dimensional coordinates of the drawing of an indoor scene to $(x', y')$ at a certain point.

$$\begin{bmatrix} x' \\ y' \end{bmatrix} = \begin{bmatrix} a_{11} & a_{12} \\ a_{21} & a_{22} \end{bmatrix} \begin{bmatrix} x \\ y \end{bmatrix} + \begin{bmatrix} t_x \\ t_y \end{bmatrix}. \qquad (3)$$

FIGURE 5: Virtual design unit 3.

When the solid model is projected, all points on any straight line on the image before and after transformation are still on a straight line after transformation, but parallel lines cannot continue to keep parallel relationship after transformation. The transformation formula of projection transformation is

$$\begin{bmatrix} x' \\ y' \end{bmatrix} = \begin{bmatrix} a_{11} & a_{12} & a_{13} \\ a_{21} & a_{22} & a_{23} \end{bmatrix} \begin{bmatrix} x \\ y \\ 1 \end{bmatrix}. \tag{4}$$

*3.2. Image Gray Interpolation.* In the image, each coordinate value is discrete, after the image transformation cannot proceed to the next step of processing. Therefore, the image gray difference algorithm is perfectly used to solve this problem. We use the common bilinear interpolation method to solve the problem, and the principle of this algorithm is shown in Figure 6.

Calculate the gray values of $E$ and $F$.

$$\begin{aligned} f(E) &= \left(x' - i\right)[f(B) - f(A)] + f(A), \\ f(F) &= \left(x' - i\right)[f(D) - f(C)] + f(C). \end{aligned} \tag{5}$$

Calculate the gray value of the fixed point.
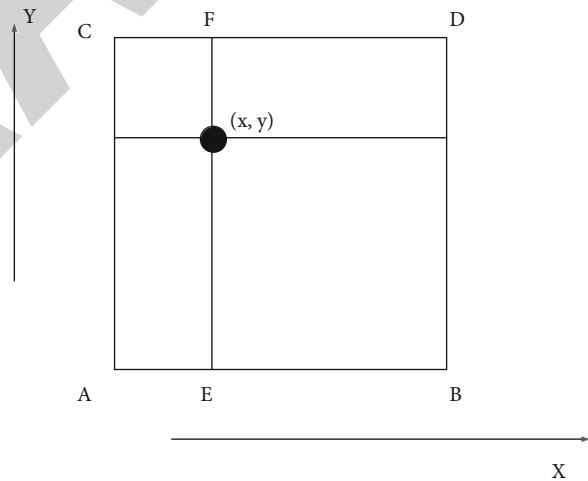
$$f(x, y) = (y - j)[f(F) - f(E)] + f(E). \tag{6}$$



FIGURE 6: Schematic diagram of image gray interpolation algorithm.

*3.3. Image Registration Algorithm.* In a virtual space scene, two coordinate points use intuitive similarity measure to measure the similarity expression.

$$\begin{aligned} D(i, j) &= \sum_{m=1}^{M} \sum_{n=1}^{m} \left[S^{i,j}(m, n)\right] - T(m, n)]^2, (i, j \in (1, N - M + 1)) \\ &= \sum_{m=1}^{M} \sum_{n=1}^{m} \left[S^{i,j}(m, n)\right]^2 - 2 \sum_{m=1}^{M} \sum_{n=1}^{M} S^{i,j}(m, n) * T(m, n) \\ &\quad + \sum_{m=1}^{M} \sum_{n=1}^{M} [T(m, n)]^2. \end{aligned} \tag{7}$$

In order to prevent the local gray intensity from affecting the registration results, the normalized cross-correlation coefficient can be used to register the similarity measure.

$$R(i.j) = \frac{\sum_{m=1}^{M}\sum_{n=1}^{m}\left[S^{i,j}(m,n) - \bar{S}\right]^2 \times \left[T(m,n) - \bar{T}\right]}{\sqrt{\sum_{m=1}^{M}\sum_{n=1}^{m}\left[S^{i,j}(m,n) - \bar{S}\right]^2}\sqrt{\sum_{m=1}^{M}\sum_{n=1}^{m}\left[T(m,n) - \bar{T}\right]^2}}. \tag{8}$$

*Principle of Nontext Matching:* in the standard image, two ROI regions are selected, one is T1 region with central coordinates $(x_1, y_1)$ and the other is T2 region with central coordinates $(x_2, y_2)$.

The angle between the connecting line of the center points of the two regions and the horizontal line is

$$\theta = \arctan g \frac{y_2 - y_1}{x_2 - x_1}. \tag{9}$$

After normalized cross-correlation single template matching, the center coordinate point is recorded, and the included angle between the connecting line of the center points of the two regions and the horizontal line is as follows:

$$\theta' = \arctan g \frac{y_2' - y_1'}{x_2' - x_1'}. \tag{10}$$

*Image Rotation Angle:*

$$\alpha = \theta' - \theta. \tag{11}$$

If the coordinates of a point on the image $f(x, y)$ to be measured are $(x, y)$, and the coordinates after theta angle rotation transformation with $(x_0, y_0)$ as the rotation center become $(x', y')$, there are

$$x' = (x - x_0)\cos\theta + (y - y_0)\sin\theta + x_0 = x^* \cos\theta + y^* \sin\theta + Dx,$$
$$y' = (y - y_0)\cos\theta + (x - x_0)\sin\theta + y_0 = y^* \cos\theta - x^* \sin\theta + Dy. \tag{12}$$

Among them

$$Dx = -x_0 \cos\theta - y_0 \sin\theta + x_0,$$
$$Dy = -x_0 \sin\theta - y_0 \cos\theta + y_0. \tag{13}$$

The registration relationship between the image to be tested $f(x, y)$ and the template image $g(x, y)$ can be modified as follows:

$$x' = x^* \cos\theta + y^* \sin\theta + Dx + \Delta x,$$
$$y' = y^* \cos\theta - x^* \sin\theta + Dy + \Delta y. \tag{14}$$

*3.4. Image Rotation Angle Detection.* The edge pixels of indoor scene are extracted by binarization, and the detected edge images are processed by binarization. If the gray image is $f(x, y)$, its average gray scale is

$$T = \frac{\sum_{i=0}^{m-1}\sum_{j=0}^{n-1}f(i,j)}{m \times n}. \tag{15}$$

The gray value of each pixel in the image is compared with the average gray value, and two sets larger than $T$ and smaller than $T$ are calculated, respectively. The formula is as follows:

$$T1 = \frac{\sum_{i=0}^{T}\text{in}_i}{\sum_{i=0}^{T}n_i},$$
$$T2 = \frac{\sum_{i=T+1}\text{in}_i}{\sum_{i=T+1}n_i}. \tag{16}$$

After Hough domain peak detection, the limit $T$ is preset.

$$T = \lambda \max A(\rho, \theta). \tag{17}$$

If the geometrical deformation between the values of $f_1$ and $f_2$ is an offset $(\Delta x, \Delta y)$, the expression is as follows:

$$f_2(x, y) = f_1(x - \Delta x, y - \Delta y). \tag{18}$$

The transformation results in

$$F_2(w_x, w_y) = e^{-j(\Delta x w_x + \Delta y w_y)} F_1(w_x, w_y). \tag{19}$$

If there is an offset in the phase spectrum $(\Delta x, \Delta y)$ Direct correlation deviation $e^{j(\Delta x w_x + \Delta y w_y)}$, i.e., if there is an offset $(\Delta x, \Delta y)$ on the phase spectrum, it is directly related to the deviation $e^{j(\Delta x w_x + \Delta y w_y)}$, that is

$$e^{j(\Delta x w_x + \Delta y w_y)} = \frac{F_1(w_x, w_y) F_2^*(w_x, w_y)}{|F_1(w_x, w_y) F_2^*(w_x, w_y)|}, \tag{20}$$

## 4. Experiment

*4.1. Simulation Experiment.* The pure text image with clothes size of 512*512 is transformed into an experimental image by transforming parameters $(\theta, \Delta x, \Delta y)$ for many times, and then the image registration experiment is carried out, and the simulation experimental results are given as shown in Table 1. The rigid transformation model is used in this paper, and the transformation parameters are $(\theta, \Delta x, \Delta y)$. The commonly used methods of image transformation model are

*Rigid Body Transformation Expression:*

$$\begin{bmatrix} x' \\ y' \\ 1 \end{bmatrix} = \begin{bmatrix} \cos\theta & -\sin\theta & t_x \\ \sin\theta & \cos\theta & t_y \\ 0 & 0 & 1 \end{bmatrix}. \tag{21}$$

Table 1: Experimental results of image registration.

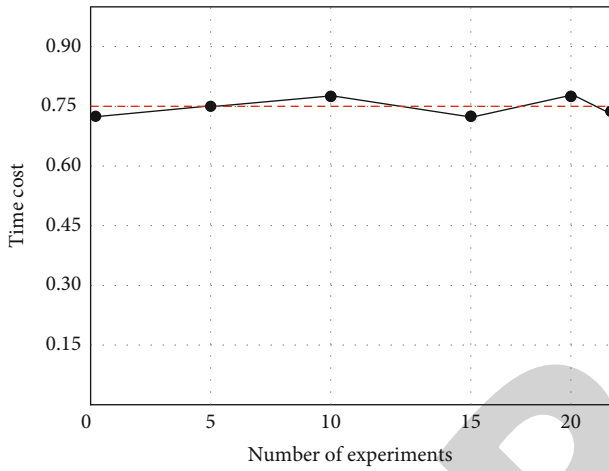| Serial number | Actual parameters | Experimental results | Time cost (s) |
|---|---|---|---|
| 1 | (4.5, 1, 1) | (4.5, 1, 1) | 0.723 |
| 2 | (4.5, 3, 3) | (4.5, 3, 2) | 0.741 |
| 3 | (4.5, 3, 2) | (4.5, 2, 2) | 0.752 |
| 4 | (-3, 3, 5) | (-3, 3, 4) | 0.786 |
| 5 | (5, 3, 1) | (5.2, 3, 1) | 0.759 |
| 6 | (2.5, 5, 6) | (3, 5, 6) | 0.781 |
| 7 | (-2.5, 2, 5) | (-3, 3, 5) | 0.757 |
| 8 | (-1, 4, 5) | (-1, 5, 5) | 0.765 |



Figure 7: Statistical chart of registration time.

*Affine Transformation Expression:*

$$\begin{bmatrix} x' \\ y' \\ 1 \end{bmatrix} = \begin{bmatrix} a_1 & a_2 & t_x \\ a_3 & a_4 & t_y \\ 0 & 0 & 1 \end{bmatrix} \begin{bmatrix} x \\ y \\ 1 \end{bmatrix}. \tag{22}$$

*Projection Transformation Expression:*

$$\begin{bmatrix} x' \\ y' \\ 1 \end{bmatrix} = \begin{bmatrix} a_1 & a_2 & a_3 \\ a_4 & a_5 & a_6 \\ a_7 & a_8 & 1 \end{bmatrix} \begin{bmatrix} x \\ y \\ 1 \end{bmatrix}. \tag{23}$$

*Nonlinear Transformation Expression:*

$$\left( x', y' \right) = F(x, y). \tag{24}$$

Through the above table, the registration results of image transformation are analyzed and counted, and the average time and cost of image transformation are obtained from the results of many experiments as shown in Figure 7.

The red horizontal line in the figure represents the average value of the time cost, which is about 0.75 s, and is obtained by averaging the time results of multiple image

Table 2: Furniture selection and placement based on convolution neural network and image transformation technology.

| Furniture selection and placement | Accuracy | Recall | F1 | Roc |
|---|---|---|---|---|
| Sofa | 98.87% | 76.87% | 76.86% | 81.25% |
| Coffee table | 97.86% | 77.54% | 73.76% | 82.35% |
| Bed | 97.54% | 76.34% | 76.52% | 83.21% |
| TV refrigerator | 96.87% | 77.28% | 77.21% | 81.61% |
| Cabinet | 95.89% | 75.81% | 75.37% | 82.57% |
| Bookcase | 96.72% | 77.29% | 75.92% | 81.78% |

Table 3: Furniture selection and placement by DBN combined with image transformation technology.

| Furniture selection and placement | Accuracy | Recall | F1 | Roc |
|---|---|---|---|---|
| Sofa | 96.57% | 64.57% | 66.66% | 71.28% |
| Coffee table | 97.84% | 66.52% | 63.56% | 73.15% |
| Bed | 96.43% | 61.24% | 64.72% | 75.31% |
| TV refrigerator | 95.17% | 67.26% | 67.26% | 72.22% |
| Cabinet | 95.22% | 65.43% | 65.45% | 73.43% |
| Bookcase | 95.12% | 63.28% | 65.52% | 74.31% |

Table 4: Furniture selection and placement based on stack self-coding network and image transformation technology.

| Furniture selection and placement | Accuracy | Recall | F1 | Roc |
|---|---|---|---|---|
| Sofa | 92.51% | 60.67% | 62.66% | 70.28% |
| Coffee table | 93.83% | 62.54% | 61.56% | 69.85% |
| Bed | 92.44% | 63.26% | 60.72% | 72.45% |
| TV refrigerator | 93.22% | 62.35% | 62.26% | 71.28% |
| Cabinet | 92.24% | 61.47% | 63.47% | 72.82% |
| Bookcase | 91.19% | 62.25% | 64.63% | 73.36% |

transformations. The average level of time response of the model is 0.75 s, so the average level of model performance can be known, and the average level of model response ability can also be described.

*4.2. Model Comparison.* In order to further improve the image transformation technology, we combine the depth learning model to optimize the technology and improve the registration accuracy of image changes. Let users get the layout design under the virtual scene conveniently and clearly and compare the model performance of indoor furniture selection and placement and vegetation landscape layout by image transformation technology under different deep learning.

When using virtual technology to select and place indoor furniture, the performance of image transformation technology combined with three different deep learning algorithms is compared, as shown in Tables 2–4.

Model performance of convolution neural network combined with image transformation technology for virtual selection and placement of furniture is shown in Figure 8.
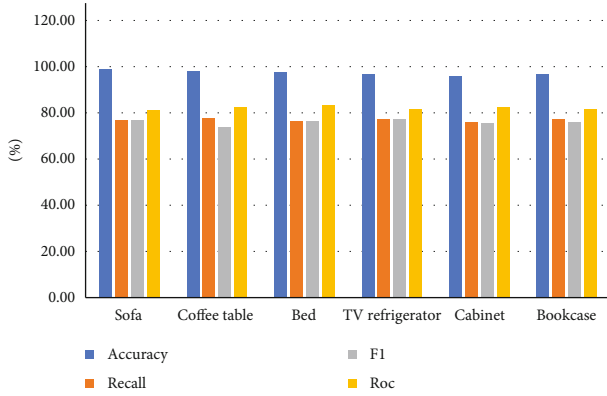
Figure 8: Performance comparison of convolution neural network combined with image transformation technology.
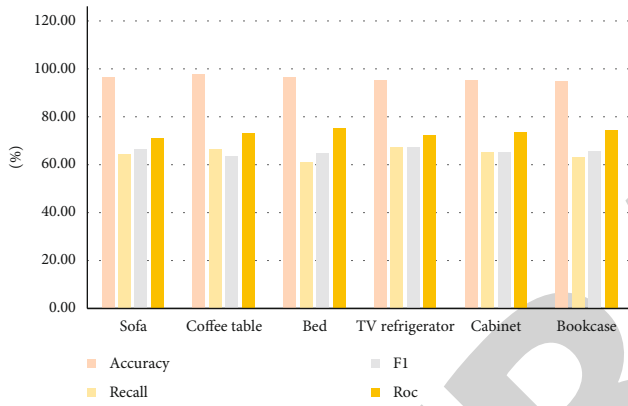


Figure 9: Performance comparison of DBN combined with image transformation technology.

Model performance of DBN combined with image transformation technology for virtual selection and placement of furniture is shown in Figure 9.

Model performance of stack self-coding network combined with image transformation technology for virtual selection and placement of furniture is shown in Figure 10.

When using virtual technology for vegetation landscape layout in different indoor areas, the performance of image transformation technology combined with three different deep learning algorithms is compared, as shown in Tables 5–7.

Convolution neural network combined with image transformation technology for performance comparison of vegetation landscape layout model in different indoor areas is shown in Figure 11.

DBN combined with image transformation technology for vegetation landscape layout model performance comparison in different indoor areas is shown in Figure 12.

Stack self-coding network combined with image transformation technology for performance comparison of vegetation landscape layout model in different indoor areas is shown in Figure 13.

4.3. Contrast Experiment. The three types of algorithms under deep learning combine image transformation technol-
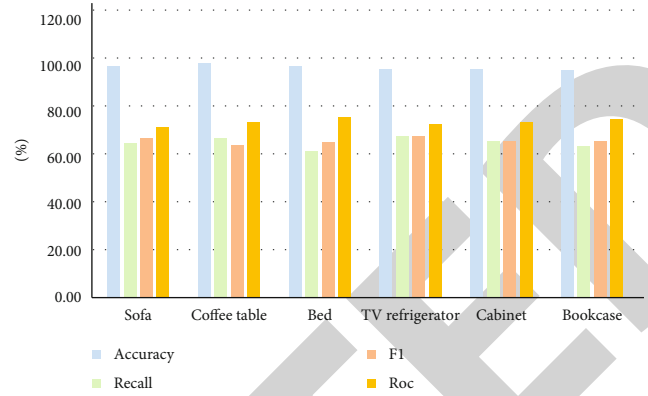


Figure 10: Performance comparison of stack self-coding network combined with image transformation technology.

Table 5: Convolution neural network combined with image transformation technology for vegetation landscape layout in different areas.

| Indoor area | Accuracy | Recall | F1 | Roc |
| --- | --- | --- | --- | --- |
| Living room | 97.89% | 82.81% | 78.88% | 83.24% |
| Balcony | 98.56% | 87.54% | 78.69% | 84.38% |
| Bedroom | 98.69% | 86.36% | 77.82% | 83.36% |
| Restaurant | 97.88% | 87.28% | 77.59% | 82.64% |
| Kitchen | 98.92% | 85.82% | 76.65% | 81.58% |
| Toilet | 97.76% | 87.23% | 77.98% | 82.48% |

Table 6: Layout of vegetation landscape in different indoor areas by DBN combined with image transformation technology.

| Indoor area | Accuracy | Recall | F1 | Roc |
| --- | --- | --- | --- | --- |
| Living room | 92.83% | 76.82% | 75.82% | 76.24% |
| Balcony | 93.52% | 77.56% | 76.64% | 75.31% |
| Bedroom | 94.65% | 76.32% | 74.82% | 78.25% |
| Restaurant | 94.83% | 77.23% | 75.54% | 77.25% |
| Kitchen | 95.32% | 75.19% | 74.68% | 77.38% |
| Toilet | 95.56% | 77.24% | 74.28% | 73.46% |

Table 7: Layout of vegetation landscape in different indoor areas by stack self-coding network combined with image transformation technology.

| Indoor area | Accuracy | Recall | F1 | Roc |
| --- | --- | --- | --- | --- |
| Living room | 92.53% | 72.85% | 72.81% | 72.25% |
| Balcony | 93.56% | 74.54% | 72.64% | 71.35% |
| Bedroom | 93.68% | 73.31% | 73.43% | 72.72% |
| Restaurant | 94.82% | 73.25% | 73.27% | 72.29% |
| Kitchen | 95.16% | 74.29% | 72.61% | 71.46% |
| Toilet | 95.27% | 73.25% | 73.49% | 72.58% |

ogy to detect and compare the image defects of indoor virtual scene layout display, carry out many experiments on virtual graphics, and count the time cost of detecting defect errors, as shown in Figure 14.
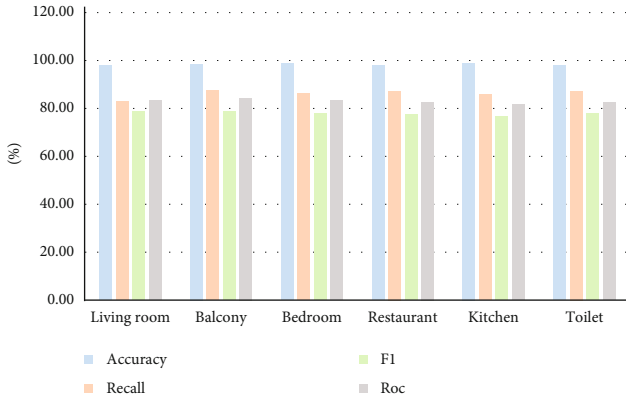
FIGURE 11: Performance comparison of convolution neural network combined with image transformation technology.
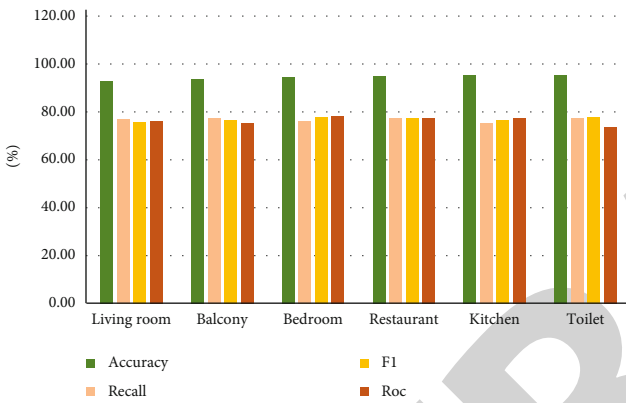


FIGURE 12: Performance comparison of DBN combined with image transformation technology.
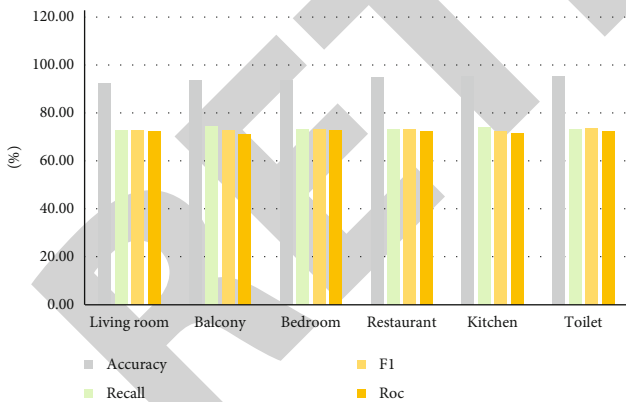


FIGURE 13: Performance comparison of stack self-coding network combined with image transformation technology.

The biggest time cost is the stack self-coding network combined with image transformation technology model. The training steps of the stack self-coding network model are divided into two steps: the first step is to design the self-coding network to initialize parameters for prelearning, and the second step is to design a classifier, and then use the classifier to fine-tune the model using the initialization
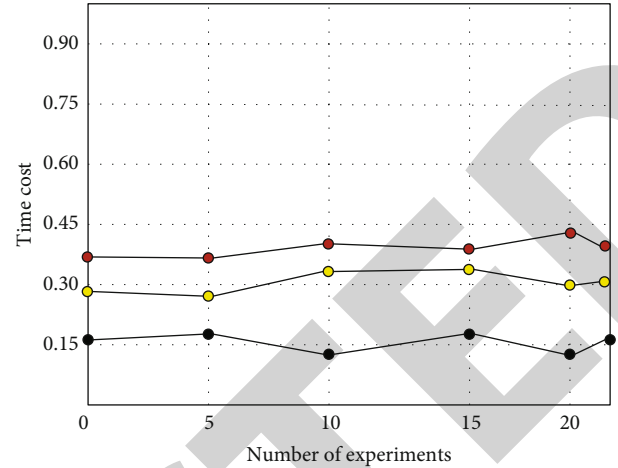


FIGURE 14: Comparison of time and cost of three optimized models.

parameters learned in the first step. Self-coding network of each layer in the learning process is

$$
\begin{aligned}
X_l &= \sigma_l^a \big( W_l^a \times X_{l-1} + b_l^a \big), \\
X_{l-1} &= \sigma_l^s \big( W_l^s \times X_l + b_l^s \big).
\end{aligned}
\tag{25}
$$

The convolution algorithm with the best performance is combined with the image transformation model: the sparse connection of the convolutional neural network has a regularization effect, which improves the stability and generalization ability of the network structure and avoids over-fitting, while the sparse connection reduces the total amount of weight parameters, which is conducive to the rapid learning of the neural network and reduces the memory overhead during calculation.

## 5. Conclusion

People's demand for 3D technology far exceeds that of 2D technology, and the application value of 3D technology is also higher. In order to analyze the virtual technology, the indoor scene is designed and analyzed. By comparing and analyzing three typical depth learning algorithms combined with image transformation technology, we get the following conclusions:

(1) In the simulation experiment, we get that the average time cost of traditional plain text image detection is about 0.75, which is much higher than that of the optimized model

(2) 3D technology realizes the best visual experience of man-machine interaction through real three-dimensional scenes and enhances realism and interactivity

(3) The selection and placement of furniture in interior landscape design takes into account the layout of the vegetated landscape, and the image transformation technology combined with convolution layer algorithm is more efficient and faster

At present, the design process of 3D design in interior design is still complex, which is different from the actual dynamic scene. In the design of different spaces, the aesthetic effect needs to be improved, and the final customer's final needs cannot be updated in time. Therefore, the further research work in the future is to solve the differences in demand from the aspects of real-time transmission and dynamic detection timeliness through the comprehensive application of 3D virtual technology and Internet of Things technology in practical application scenarios.

## Data Availability

The experimental data used to support the findings of this study are available from the corresponding author upon request.

## Conflicts of Interest

The authors declared that they have no conflicts of interest regarding this work.

## References

[1] M. Sander, "Digital 3D technologies for humanities research and education: an overview," *Applied Sciences*, vol. 12, no. 5, pp. 2426–2426, 2022.

[2] H. Luo, Z. Yiren, and Y. Li, "Research on virtual campus roaming system based on unity 3D technology," *Journal of Physics: Conference Series*, vol. 2173, no. 1, article 012039, 2022.

[3] N. M. Truong, V. T. Thuy, and N. Q. Ngoc, "Advanced digital 3D technology in the combined surgery-first orthognathic and clear aligner orthodontic therapy for dentofacial deformity treatment," *PRO*, vol. 9, no. 9, pp. 1609–1609, 2021.

[4] M. Skublewska-Paszkowska, M. Milosz, P. Powroznik, and E. Lukasik, "3D technologies for intangible cultural heritage preservation—literature review for selected databases," *Heritage Science*, vol. 10, no. 1, pp. 3–3, 2022.

[5] S. Liu, Y. Tu, X. Wang et al., "Transparent reversible prosthesis, a new way to complete the conservation–restoration of a Black Ding Bowl with application of 3D technologies," *Heritage Science*, vol. 10, no. 1, 2022.

[6] S. Li, "Ancient Architecture Animation Design Method of 3D Technology and Its Application," *Journal of Physics: Conference Series*, vol. 2037, no. 1, 2021.

[7] F. Darjan and M. Josip, "Value of 3D-DSA in the detection of intracranial aneurysms: the comparison of 3D technique and digital subtraction angiography," *Medicina Fluminensis : Medicina Fluminensis*, vol. 57, no. 3, pp. 260–268, 2021.

[8] P. Derudas and Å. Berggren, "Expanding field-archaeology education: the integration of 3D technology into archaeological training," *Open Archaeology*, vol. 7, no. 1, pp. 556–573, 2021.

[9] A. Engleman, "Designing structures that test and optimize recruitment: coral restoration using innovative 3D technology," *Journal of Coastal Zone Management*, vol. 24, no. 5, pp. 2–2, 2021.

[10] M. H. Seo, H. J. Yang, J. J. Han, I. J. Kwon, H. Myoung, and S. M. Kim, "Surgical repositioning of an inverted developing incisor assisted by 3D technology," *Applied Sciences*, vol. 11, no. 11, pp. 4827–4827, 2021.

[11] H. Tan, E. Huang, X. Deng, and S. Ouyang, "Application of 3D printing technology combined with PBL teaching model in teaching clinical nursing in congenital heart surgery: a case-control study," *Medicine*, vol. 100, no. 20, 2021.

[12] P. Moreau, S. Ismael, H. Masadeh et al., "3D technology and telemedicine in humanitarian settings," *The Lancet Digital Health*, vol. 2, no. 3, pp. e108–e110, 2020.

[13] F. Edouard, "Impact of 3D technology on vision," *Actualites Pharmaceutiques*, vol. 59, no. 594, pp. 11–11, 2020.

[14] L. C. Davis, J. Tomlinson, L. Khoza, and N. Jamaludeen, "Collaboration of 3D technology and fashion innovations: a creative accessory development assessment," *Fashion, Style & Popular Culture*, vol. 7, no. 2-3, pp. 179–191, 2020.

[15] X. Willis, X. Ding, J. Singleton, and F. F. Balakirev, "Cryogenic goniometer for measurements in pulsed magnetic fields fabricated via additive manufacturing technique," *The Review of Scientific Instruments*, vol. 91, no. 3, 2020.

[16] H. Quan, T. Zhang, H. Xu, S. Luo, J. Nie, and X. Zhu, "Photocuring 3D printing technique and its challenges," *Bioactive Materials*, vol. 5, no. 1, pp. 110–115, 2020.

[17] X. Zhang, J. Zhou, and Y. Xu, "Experimental study on preparation of coaxial drug-loaded tissue-engineered bone scaffold by 3D printing technology," *Proceedings of the Institution of Mechanical Engineers, Part H: Journal of Engineering in Medicine*, vol. 234, no. 4, pp. 309–322, 2020.

[18] M. Jaumotte, P. Grobet, F. Pepinster, F. Thonnart, J. L. Nizet, and Y. Gilon, "Contribution of 3D technology for maxillofacial surgery," *Revue Medicale de Liege*, vol. 75, no. 4, pp. 240–242, 2020.

[19] D. Garrett, "Patient-specific 3D-printed rhinoplasty operative guides," *The American Journal of Cosmetic Surgery*, vol. 37, no. 3, pp. 143–147, 2020.

[20] N. A. Bushmeleva, N. I. Isupova, E. A. Mamaeva, and E. V. Kharunzheva, "Peculiarities of engineering thinking formation using 3D technology," *European Journal of Contemporary Education*, vol. 9, no. 3, pp. 529–545, 2020.

[21] R. Wilk, W. Likus, A. Hudecki, M. Syguła, A. Różycka-Nechoritis, and K. Nechoritis, "What would you like to print? Students' opinions on the use of 3D printing technology in medicine," *PLoS One*, vol. 15, no. 4, 2020.

[22] J. K. Schwartz, A. Fermin, K. Fine et al., "Methodology and feasibility of a 3D printed assistive technology intervention," *Assistive Technology*, vol. 15, no. 2, pp. 141–147, 2020.

[23] G. S. Shin, H. K. Kweon, Y. G. Kang, and W. T. Oh, "Ceramic direct rapid tooling with FDM 3D printing technology," *Journal of the Korean Society of Manufacturing Process Engineers*, vol. 18, no. 7, pp. 83–89, 2019.

[24] X. Peiying, "Study on the correlation parameters of class II malocclusion in child tooth dentition early stage by using 3D technique," *Pakistan Journal of Medical Sciences*, vol. 35, no. 5, pp. 1290–1294, 2019.

[25] E. Honkavaara, K. Karantzalos, X. Liang, E. Nocerino, I. Pölönen, and P. Rönnholm, "Editorial for the special issue "frontiers in spectral imaging and 3D technologies for geospatial solutions"," *Remote Sensing*, vol. 11, no. 14, pp. 1714–1714, 2019.